Respiration Physiology (1982) **49**, 75–95
Elsevier Biomedical Press

A MODEL STUDY OF FLOW DYNAMICS IN HUMAN CENTRAL AIRWAYS. PART I: AXIAL VELOCITY PROFILES

H. K. CHANG and OSAMA A. EL MASRY*

Biomedical Engineering Unit and Department of Physiology, McGill University, Montreal, Quebec, Canada

Abstract. We measured detailed steady inspiratory and expiratory velocity profiles in a 3:1 scale model of the human central airways. The model was constructed out of acrylic plastic, mounted vertically, and connected to a specially designed steady-flow system. Laterally introduced hot-wire anemometer probes were used to record axial velocities along 4 diameters at each of the 12 pre-drilled stations of measurement; the flow distribution among the five lobar bronchi was controlled by distally positioned linear resistors. Whether with a flat entrance profile or entering as a narrow jet, the inspiratory flow velocity profiles in the frontal plane showed a high degree of asymmetry in all branches, with peak velocities near the inner wall of the bifurcation. In the sagittal plane the velocity profiles were nearly symmetric, exhibiting a single peak near the center in the frontal plane and almost flat in the sagittal plane. Overall, the velocity profiles were more sensitive to airway geometry than to flow rate. The only site of flow separation was observed in the right upper lobar bronchus. The most evident modification of axial velocity profiles in a single branch was found in the left main bronchus during expiratory flow.

Air flow patterns
Airway model
Bronchial tree
Fluid mechanics
Hot-wire anemometry
Quasi-steady flow
Velocity profiles

Knowledge of air flow characteristics in the tracheo-bronchial tree is essential to the understanding of airway resistance, intrapulmonary gas mixing and deposition of airborne particles. To gain such knowledge, techniques of bronchial catheterization in the large airways have been developed. However, in addition to the inconveniences, the presence of the catheter in the airways necessarily distorts the airway geometry as well as the flow dynamics. It is also impossible to measure detailed velocity distribution with this technique.

Accepted for publication 2 March 1982

Technical assistance was afforded by Christopher H. Bracken.

* Present address: Department of Mechanical Engineering, University of Alexandria, Alexandria, Egypt.

A practical alternative to *in vivo* measurement is the study of physical models or lung casts. In this regard, the work by Schroter and Sudlow (1969) has provided valuable information. These authors studied the steady-flow velocity profiles in symmetric bifurcation models and showed that for Reynolds numbers of 300–700 the axial velocity profiles were highly skewed. Schreck and Mockros (1970) have also obtained a series of axial velocity profiles in a single bifurcation for Reynolds numbers under 2400. Olson *et al.* (1973), on the other hand, have measured mean steady-flow velocity at different positions of a lung cast. Motivated by an interest in arterial blood flow, El Masry *et al.* (1978) investigated the streamline patterns and flow separation in bifurcation models under different flow conditions. In two reviews of pulmonary fluid dynamics (Pedley, 1977; Pedley *et al.*, 1977) extensive citation was made of an unpublished thesis by Olson (1971) who apparently was first to measure secondary flow in bifurcating tubes. All the above-cited work was made in one- or two-generation idealized bifurcations; the asymmetry of the bronchial tree was neglected. We have, however, constructed a four-generation asymmetric model of the human central airways in accordance with the lung geometry reported by Horsfield *et al.* (1971). Our purpose was to provide quantitative information concerning flow dynamics in the human central airways. In this paper, we present the steady axial velocity profiles. In the companion paper (Isabey and Chang, 1982) the secondary flow characteristics in this airway model are reported. The velocity profiles during oscillatory flows will be described in Part III of this sequence of studies (Menon *et al.*, 1982).

Apparatus and methods

PHYSICAL MODEL

As shown in fig. 1, a 3:1 scale rigid model of the first 3–4 generations of human central airways from the trachea to the five lobar bronchi was constructed from blocks of clear acrylic plastic (Perspex) and circular tubes. Power drilling as well as manual forming were used to shape the transition sections and flow dividers of the various bifurcations; all flow dividers were carefully made sharp so as to resemble the healthy human airways. The four transparent blocks were jointed together with heat-treated curved tubes such that the dimensions of this model were consistent with the lung geometry reported by Horsfield *et al.* (1971). The final dimensions of this model as well as those given by Horsfield are compared in table 1, with fig. 2A providing a key to the numbering system of the various branches.

Fig. 1. (A) Front view of the human central airway model. With a 3:1 scale, the model has internal dimensions which conform to the lung geometry given by Horsfield *et al.* (1971). (B) Side view of a conic diffuser and a linear resistor which were attached to the terminal airways of the model.

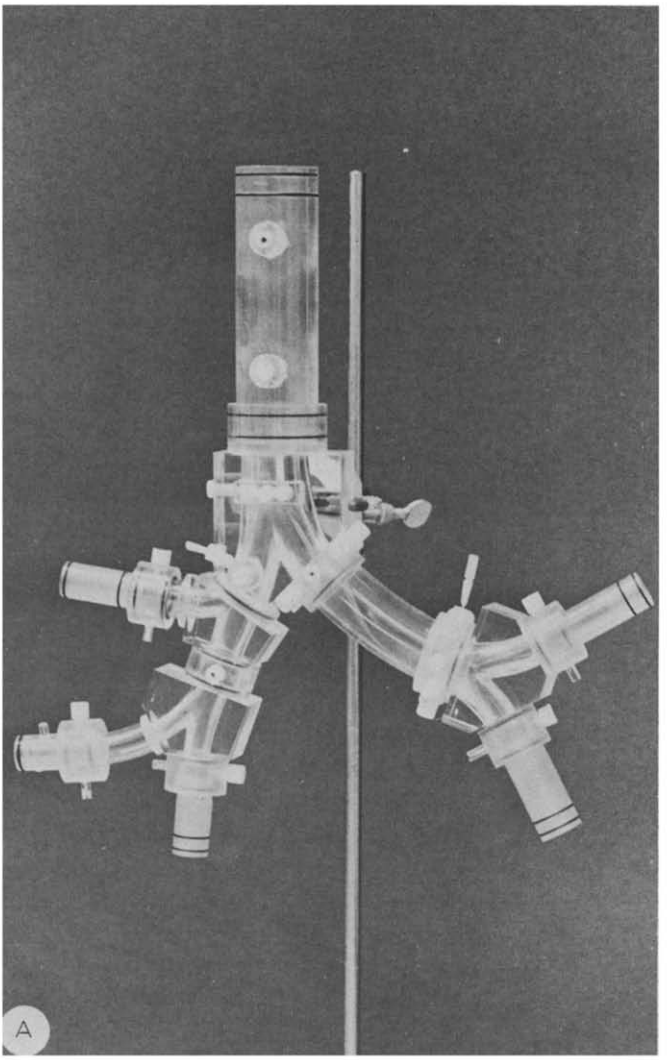
A

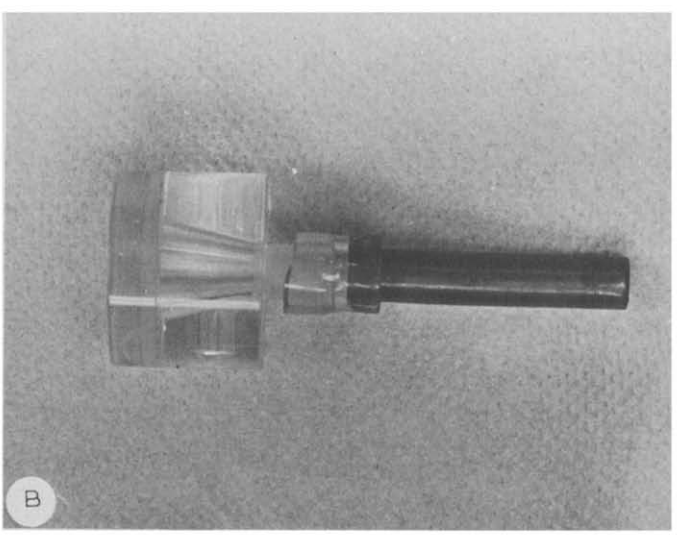
B

TABLE 1.
Comparison of the Horsfield airway model and the present model

Branch No.	Horsfield airway model*				Present model***		
	Diameter d_A (mm)	Length l_A (mm)	Angle (deg)	Radius of curvature R**	Branch designation	Diameter d_M (mm)	Length l_M (mm)
0	16.00	100.00	0.0	∞	a	47.6	299.0
1	12.00	50.00	73.00	54.0	b	34.6	155.0
10	11.10	22.00	35.00	33.3	c	34.0	54.9
2	7.50	16.00	48.00	26.3	d	22.1	51.8
6	8.00	11.00	44.00	50.0	e	23.2	33.8
13	8.90	26.00	15.00	20.5	f	25.8	80.2
11	7.30	15.60	63.00	12.4	g	21.8	51.6
15	6.40	8.00	15.00	37.8	h	18.4	26.4
14	5.20	21.00	61.00	41.6	i	15.4	66.0

* Dimensions given here pertain to 75% TLC.
** Mean radius of curvature in the frontal plane.
*** Branching angles and mean radii of curvature conform to the Horsfield model, but slight local modifications were necessary to provide smooth transitions from one branch to another.

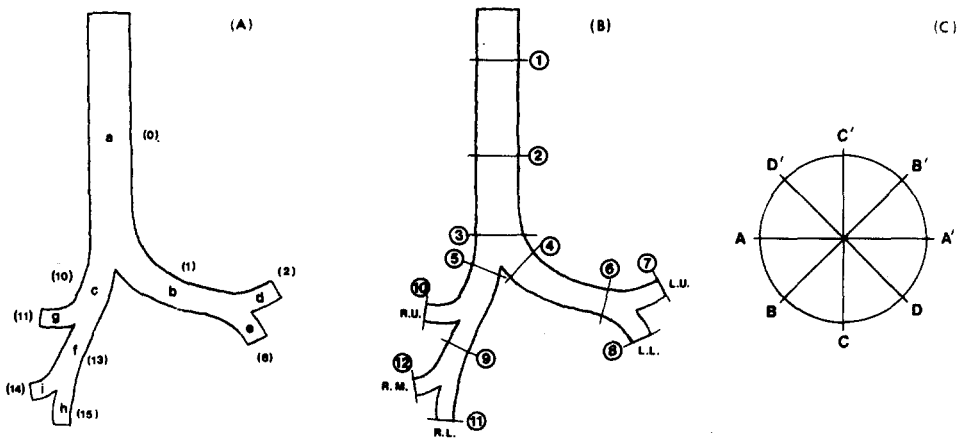

Fig. 2. (A) Sketch of the airway model. The individual airways as designated by Horsfield *et al.* (1971) are given by the numerals in parentheses and the lower case letters are the designation used for the present model. Dimensions of both the Horsfield lung model and the present model are given in table 1. (B) Sketch of the model with the locations of the 12 stations of velocity measurement; detailed dimensions and distances are given in table 2. (C) Cross-section of a measurement station viewed from a more proximal position. Velocity profiles were obtained along 4 diameters. Diameter A–A′ is always in the frontal plane (plane of bifurcation) and diameter C–C′ in the sagittal plane (plane normal to bifurcation), with C′ always on the ventral side. Points A,B,C,D rotate counterclockwise.

Lateral ports were provided at 12 cross-sections to allow the introduction of the measuring probe. The locations and numbering of these 12 stations are shown in fig. 2B in conjunction with table 2. At each of the 12 stations (except station 3 which was not circular but elliptic) provision was made to allow the measuring probe to transverse at least four equally spaced diameters, as shown in fig. 2C.

This model being of 3:1 scale in relation to the human airways, the principle of dynamic similarity must be observed. In the air flow problem which interests us, it is sufficient to require the equality of Reynolds number in the model and the airways (Daily and Harleman, 1966), *i.e.*,

$$\frac{U_M L_M}{\nu_M} = \frac{U_A L_A}{\nu_A} \tag{1}$$

In eq. (1) U denotes linear velocity, L denotes linear dimension, ν is the fluid kinematic viscosity and the subscripts M and A signify model and airway, respectively.

Since air was used as the experimental gas, $\nu_A = \nu_M$; hence, we have

$$\frac{U_M}{U_A} = \frac{L_A}{L_M} = \frac{1}{3} \tag{2}$$

Equation (2) means that the linear velocity measured in the model is one-third of that in the airways at an identical Reynolds number. To avoid possible confusion in conversion, all velocity magnitudes reported in this paper are normalized by the

TABLE 2
Locations of the stations of measurement

Station No.	Branch	Diameter d (mm)	Nearest proximal bifurcation	Distance from bifurcation l** (mm)	l/d
1	a	47.6	Tracheal*	222	4.7
2	a	47.6	Tracheal*	132	2.8
3	a	47.6	Tracheal*	48	1.0
4	b	34.6	Tracheal	30	0.9
5	c	34.0	Tracheal	17	0.5
6	b	34.6	Tracheal	135	3.9
7	d	22.1	Left lower	49	2.2
8	e	23.2	Left lower	39	1.7
9	f	25.8	Right upper	36	1.4
10	g	21.8	Right upper	51	2.3
11	h	18.4	Right lower	32	1.7
12	i	15.4	Right lower	81	5.3

* Stations proximal to carina.

** Measured from center of carina, along center line of airway.

mean velocity over the cross-section and only Reynolds numbers will be used to indicate velocity magnitudes.

FLOW RATES AND DISTRIBUTIONS

Two steady tracheal flow rates were used in this study: 5.0 L/sec and 1.2 L/sec, which according to eq. (1) correspond to 1.66 L/sec and 0.40 L/sec in the real lung.

The tracheal flow was distributed among the five lobar bronchi according to the approximate lobar volumes at 75% TCL as reported by Horsfield *et al.* (1971) The exact percentages of tracheal flow received by each lobar bronchi were checked by summing the velocities (see below) over the corresponding stations and are given in table 3. Although this estimation was subject to some errors, the sum of the five lobar flows obtained this way was always within 10% of the measured tracheal flow.

To ensure the desired flow distribution at different flow rates, linear resistors made of copper tubes (10 mm ID) of various lengths, each packed with 35 steel capillary tubes (1.2 mm ID), were used distal to the terminal airways. Five identical plastic conic diffusers provided the transition from the terminal airways of the model to these resistors (fig. 1B). Since the resistance of these resistors were many times greater than the large-bore airways of the model, the distribution of tracheal flow was entirely determined by the relative lengths of the linear resistors.

To simulate severe obstruction of a lobe, an extra-long resistor was used in the right lower lobar bronchus. The resulting flow distribution was again obtained by integration of the linear velocities.

FLOW SYSTEM

The tracheal flow rate during both inspiratory and expiratory flow was controlled with a precision metering valve (Whitey SS-3LR4) and measured with a flowmeter (Brooks 1307 No. 8 or 9) calibrated to have an accuracy of $\pm 1\%$ of the maximum

TABLE 3

Distribution (%) of flow in this study as compared to static lung volume at 75% and the Horsfield lung model

Lobe	Right upper	Right middle	Right lower	Left upper	Left lower	Total
Static lung volume at 75%*	19	10	26	19	26	100
Horsfield lung model	21	9	25	20	25	100
Present study	20	10	25	20	25	100

* As reported by Horsfield *et al.* (1971).

reading. To avoid damaging and influencing the reading of the hotwire probe, air was passed through an air filter (0.8 μm pore size) before reaching the model. For inspiratory flow experiments, a large drum-like reservoir (30 cm ID × 35 cm high) was used proximal to the model. The reservoir had a double-layer stainless-steel wire mesh to stabilize the flow and to damp out any large-scale fluctuations emanating from the air stream. During expiratory flow, air passed from the filter to a central manifold (11 cm ID × 22 cm high) with five outlets. Tygon tubings were used to connect these outlets and the five resistors distal to the lobar bronchi. The fine capillaries in these resistors (minimum length 6 cm) served as flow stabilizers in this case, and the lid of the reservoir was opened to provide flow exit.

To simulate glottic aperture, a narrow (1.6 cm) slit located centrally in the anterior–posterior direction was constructed at the junction of the trachea and the drum-shaped reservoir. Velocity profiles were measured either with this slit or with a full opening at the proximal end of the trachea.

VELOCITY MEASUREMENT

A constant temperature anemometer system (Disa 55M01) was used to measure the axial velocity at different positions in the model. A specially made miniature right-angle probe was entered in the model laterally from a pre-drilled port. The sensor of the probe was made of platinum-plated tungsten wire (5 μm in diameter with a functional length of 1.25 mm) and was placed in the flow field perpendicular to the axial flow direction. Due to the different cooling effect by different velocities on the hot-wire sensor, the anemometer system gave different output signals. These signals were then passed through a linearizer (Disa 55M25) which was adjusted to yield a linear output of the voltage–velocity relationship. A digital voltmeter (Disa 55D31) was used to read out the average local velocity over a pre-set time interval.

The hot-wire probe was calibrated by means of a horizontal straight tube 0.928 cm in diameter and 180 cm in length. By keeping the Reynolds number in the tube well below 2000, the flow was Poiseuille and the velocity profile issuing from the downstream end of the tube was parabolic. Using a sensitive differential pressure transducer (Validyne DP103) to measure the lateral pressure drop over a 50 cm length near the downstream end of the tube, the flow rate and therefore the magnitude of the peak velocity of a given parabolic profile could be easily computed from Poiseuille's law. This was additionally verified by comparing the flow rates computed from the pressure drops with those measured directly with volumetric flowmeters (Brooks Sho-Rate 150 series). Being positioned immediately downstream of the tube exit and at the center of the circular cross-section, with the aid of a micromanipulator, the hot-wire probe was therefore always sensing the peak velocity of the parabolic profile within the accuracy defined by the length (1.25 mm) of the measuring probe. For the range of flow rates considered, this was estimated to be about 95% accurate. By relating the computed peak velocity and the voltage output of the hot-wire probe, the latter was calibrated for actual measurement in the airway model.

Steady-flow axial velocities were measured at 12 stations, along 4 equally-spaced diameters at each station and at 17 points along each diameter. The 17 positions along a given diameter were not evenly spaced, but were so arranged that the 8 annuli defined by connecting the corresponding points along the 4 diameters in the circular cross-section had identical areas; thus the points were loosely spaced near the the center of the airway and increasingly more closely spaced toward the airway wall where velocity gradient was generally greater. The manner in which these 65 points of measurement were distributed in a cross-section permitted the division of a given cross-section into 65 small regions of equal area, each with a representative velocity. Thus the flow rate passing a cross-section could be easily estimated by summing the axial velocities at the 65 points of measurement. Indeed it was this simple method of integration which allowed for the calculation of flow distribution. This method of flow estimation was subject to some errors, notably the inaccuracy of the velocities measured near the wall and the small but perhaps non-zero contribution of either tangential or radial (but not both) velocity components to the overall cooling of the hot-wire sensor. The results thus yielded, however, were satisfactory when compared with direct flow measurements; the accuracy was not much lower than the 95% accuracy of the probe calibration.

Results

Two physiological flow rates (0.4 L/sec and 1.7 L/sec) were studied; the Reynolds numbers as well as the mean velocities in the 9 branches of the model are given in table 4. Some selected axial velocity profiles are presented below.

TABLE 4
Reynolds numbers and mean velocities in the model

Branch	Station No.	% Flow	$\dot{V}_M$ = 1.2 L/sec		$\dot{V}_M$ = 5.0 L/sec	
			Re	U (cm/s)	Re	U (cm/s)
a	1,2	100	2123	67.3	8846	337.2
b	4,6	45	1329	57.4	5537	287.2
c	5	55	1635	72.7	6811	363.5
d	7	20	915	62.6	3812	312.8
e	8	25	1089	71.0	4538	354.8
f	9	35	1371	80.3	5712	401.7
g	10	20	927	64.3	3862	321.5
h	11	25	1373	112.8	5714	564.1
i	12	10	656	64.4	2734	322.1

INSPIRATORY FLOW

Figure 3 shows three sets of axial velocity profiles in the trachea (Stations 1 and 2) obtained from two entrance conditions at two flow rates. The tracheal flow rates refer to the equivalent physiological flows, the positions of the stations are marked in the sketch of the model, and the two profiles for each station are the ones in the frontal plane (A–A′) and in the sagittal plane (C–C′) with the positions of A and A′ also marked in the model sketch. In each panel the abscissa indicates dimensionless radial position with A (or C) corresponding to the extreme left position in the panel. The ordinate of each panel represents linear velocity normalized by the mean velocity over the cross-section.

Figure 3 indicates that the standard entering profile in the trachea of the model was fairly flat and was beginning to develop into a parabolic shape due to viscous effects which were gradually propagated toward the center of the airway. On the other hand, the profile resulting from a slit entrance exhibited the characteristics of a jet. At Station 1, due to the anterior–posterior direction of the slit, the C–C′ profile was much broader than that in the A–A′ diameter. But this jet seemed to have diffused quickly into a round jet, as is evidenced by the near axisymmetry of the velocity profiles at Station 2.

Three sets of profiles obtained at Station 4 immediately downstream of the tracheal bifurcation are shown in fig. 4, each set consisting of 4 profiles along 4 diameters. Here the profiles from a slit entrance and from a round entrance were both skewed

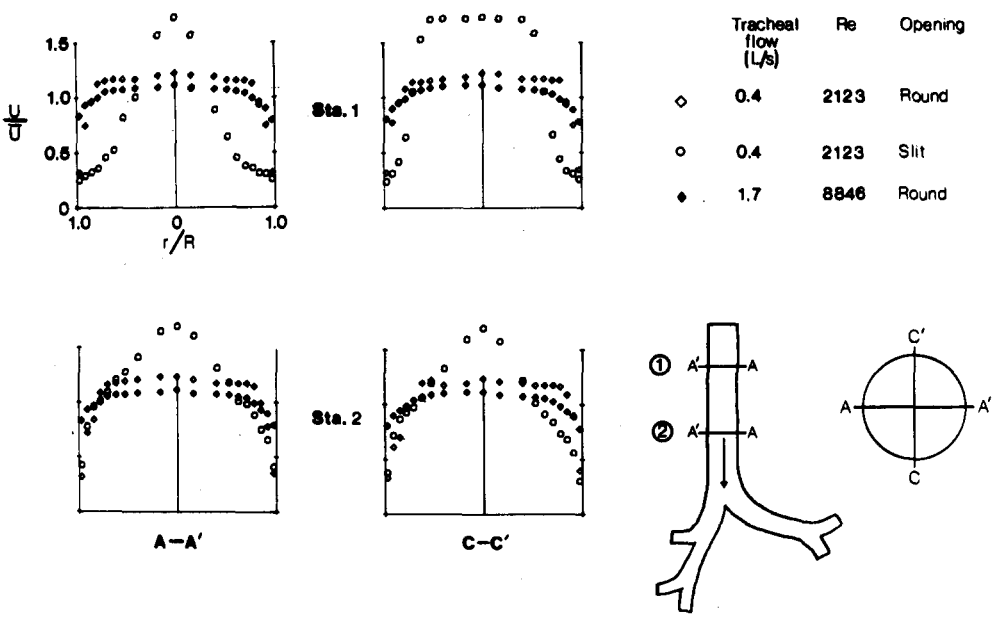

Fig. 3. Axial velocity profiles in the trachea (Stations 1,2). Inspiratory flow at two flow rates and two entrance conditions.

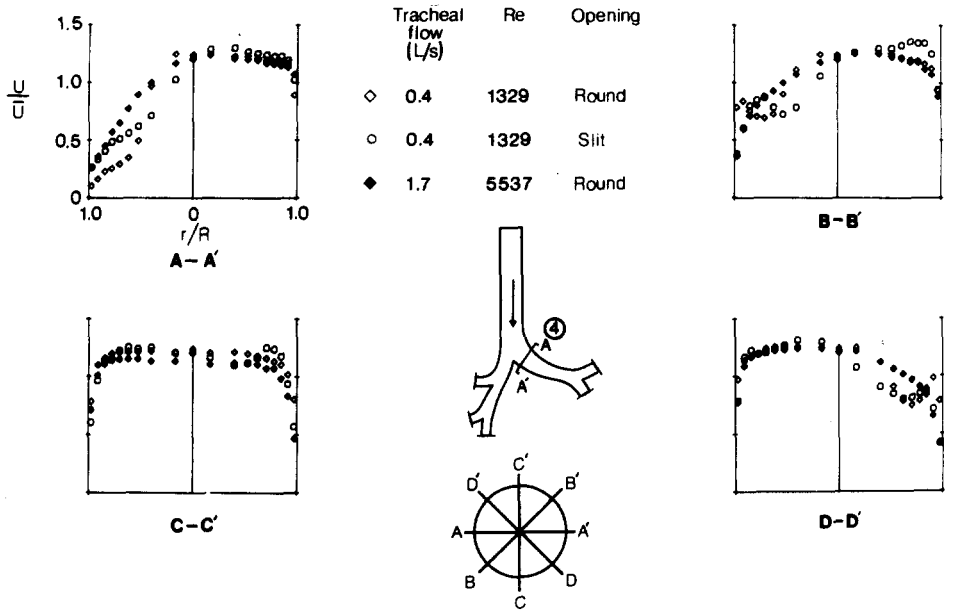

Fig. 4. Axial velocity profiles in the proximal part of left main bronchus (Station 4). Inspiratory flow at two flow rates.

and less distinct from each other. Namely, after a single bifurcation, the centrifugal force and the development of new boundary layers predominated and the shape of the entering velocity profiles became secondary. The velocity profiles obtained at Re = 5537 have basically similar configurations to those at Re = 1329.

Further downstream in the left main bronchus (Station 6), the axial velocity profiles developed into a basically bi-peak structure (fig. 5). At Re = 1329, the profile in the frontal plane (A–A′) has a high peak near the central wall (A′) and a much lower peak near the lateral wall (A); the profile in the sagittal plane (C–C′) is almost symmetric. At a higher Reynolds number (5537) when the flow was most likely turbulent, the profiles exhibited essentially the same characteristics. The only difference is that the peaks of these profiles were more moderate than those at Re = 1329, likely in the laminar flow regime. This moderation of the peaks can be explained by the transverse momentum exchange associated with higher Reynolds number flows, and this is also probably why the profiles given by Schroter and Sudlow (1969), who studied much lower Reynolds numbers than we did, appeared even more drastic than those shown here.

The velocity profiles in the left upper (Station 7) and lower (Station 8) lobar bronchi are shown in fig. 6. After two bifurcations the velocity profiles in the frontal plane were still skewed toward the inner wall of the bifurcation and the profiles along the C–C′ diameter were nearly symmetric with a mild bi-peak structure. At Station 7 the air particles had made two consecutive turns in the same direction,

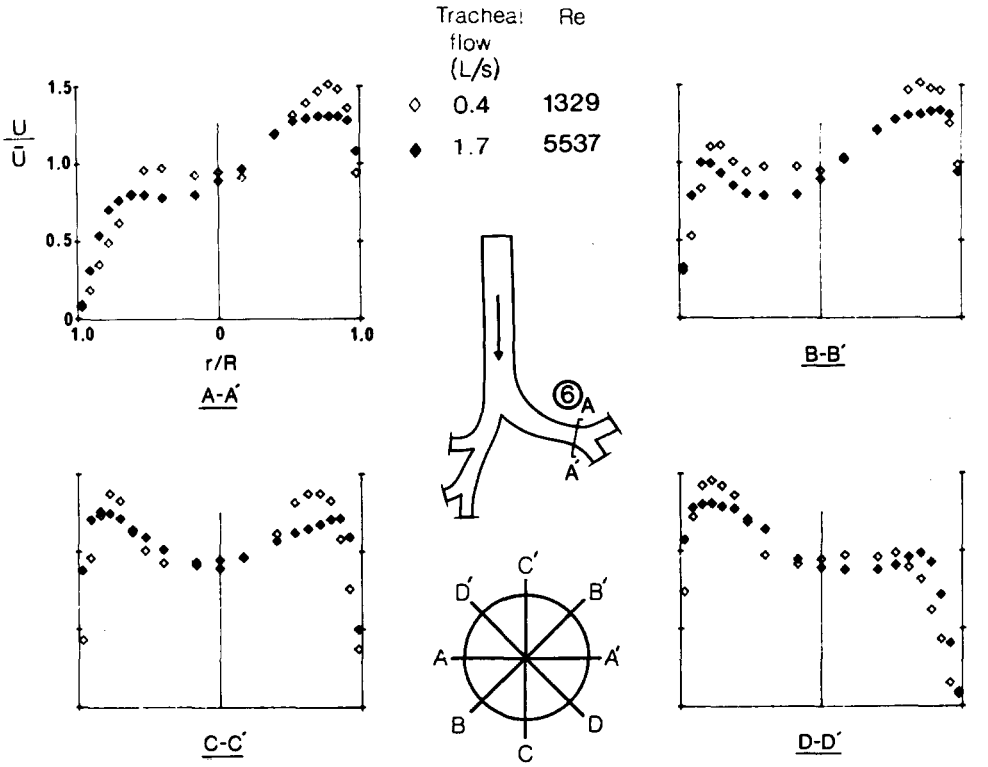

Fig. 5. Axial velocity profiles in the distal part of the left main bronchus (Station 6). Inspiratory flow at two flow rates.

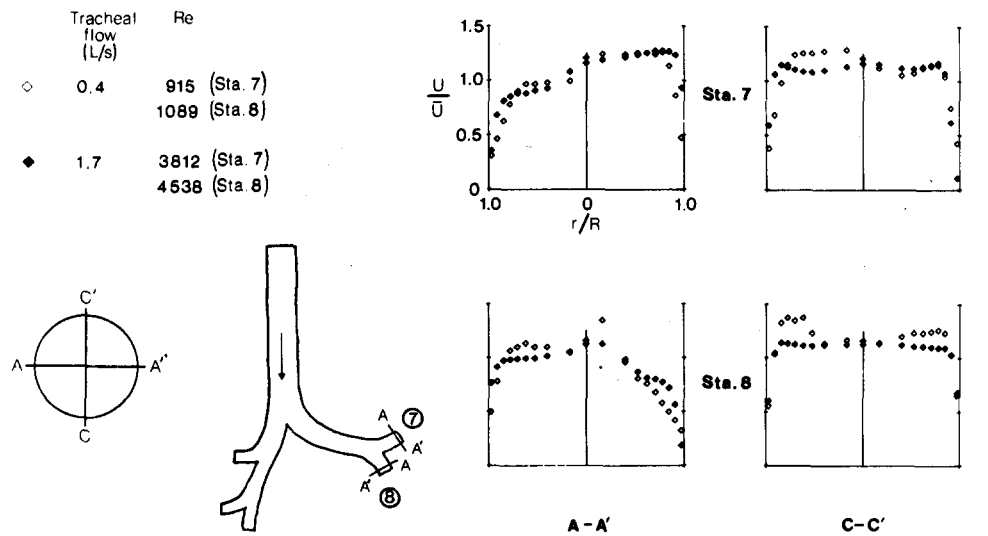

Fig. 6. Axial velocity profiles in left upper lobar bronchus (Station 7) and left lower lobar bronchus (Station 8). Inspiratory flow at two flow rates.

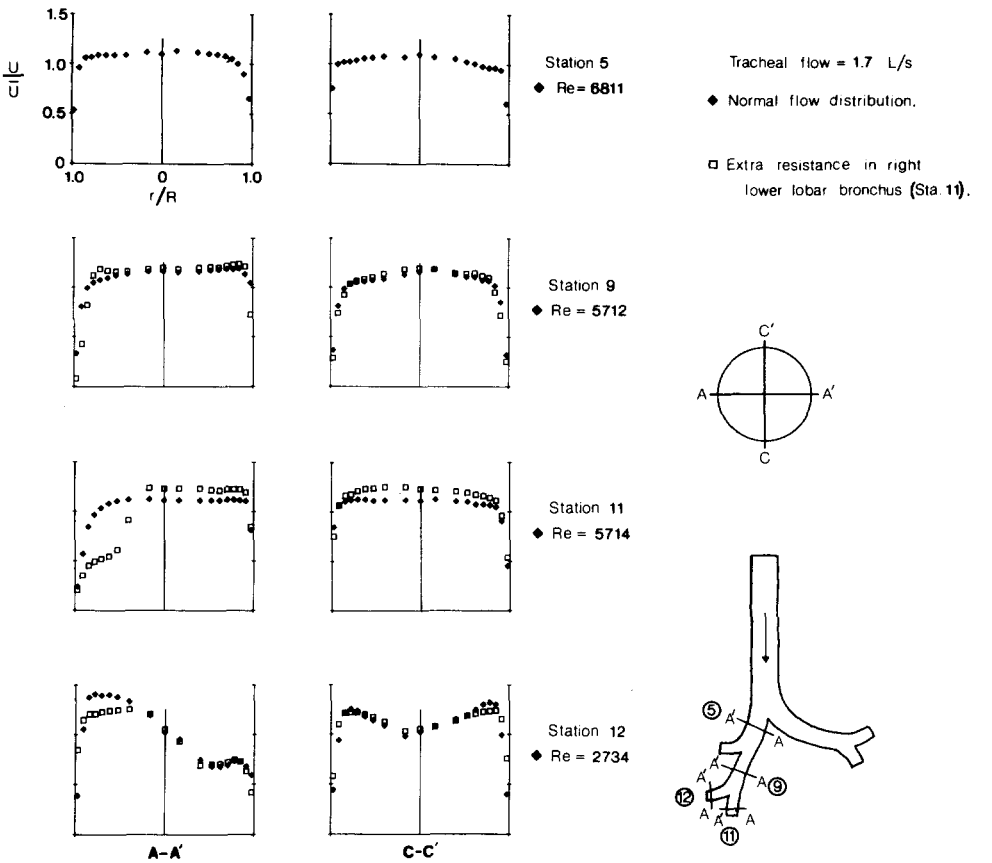

Fig. 7. Axial velocity profiles in the right main bronchus (Stations 5,9) as well as in the right middle (Station 12) and lower (Station 11) lobar bronchi. Two flow distributions were studied.

whereas at Station 8 the air had experienced two turns in the opposite direction. Despite this difference in history, the skewedness of the velocity profiles was of similar degree, indicating again that the influence of the immediate bifurcation, *i.e.*, centrifugal force and development of new boundary layers, was much stronger than the entering velocity profile in shaping the ensuing flow.

Four sets of velocity profiles at a tracheal flow rate of 1.7 L/sec in the right lung are presented in fig. 7. The velocity profiles in the right main bronchus (Station 5) were fairly blunt and almost symmetric on account of the mild branching angle. After the branching off of the right upper lobar bronchus, the velocity profiles at Station 9 were still nearly symmetric, again due to the basically straight airway. Thus, despite repeated branching, the profiles in the right middle and lower lobar bronchi (Stations 12 and 11, respectively) were not very different from those after a single bifurcation. The velocity profiles obtained at 0.4 L/sec (not shown) were quite similar to those shown in fig. 7.

To simulate the effect of severe obstruction of a lobe, we applied an extra-long linear resistor to the right lower bronchus. Figure 7 also shows the frontal plane (A–A′) and sagittal plane (C–C′) velocity profiles at three stations (Stations 9,11,12). The increased resistance at Station 11 reduced its flow by about a half and increased the flow at Station 12 (also at Station 10) moderately. Since Station 9 governed the flow to the right middle and lower lobes, its flow was reduced by about a quarter. Despite these changes in Reynolds number, the velocity profiles were almost superimposable on those obtained at the regular flow distribution.

The most interesting velocity profiles were observed in the right upper lobar bronchus (Station 10) which branches off the right main bronchus at a very sharp angle. Shown in fig. 8 are two sets of profiles corresponding to the two flow rates used (Re = 927 and 3862). Quantitatively, these profiles are somewhat like a mirror image of those at Station 6 (fig. 5), including the fact that the profiles for the laminar flow have more pronounced peaks. It is intersting to note that the profile in the A–A′ diameter at Re = 927 has a zone of 'zero' flow whereas the corresponding velocities for Re = 3862 are considerably higher. The recorded 'zero' flow was likely in the zone of flow separation or mild reverse flow (Daily and Harleman, 1966). Since the flow at Re = 3862 was most likely turbulent and carried with it a great

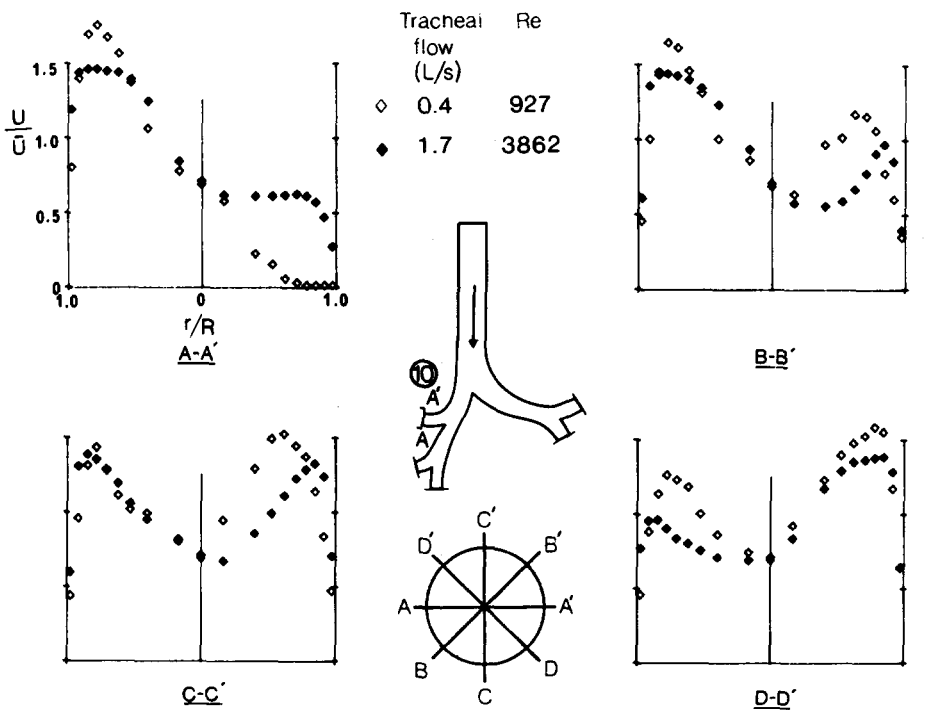

Fig. 8. Axial velocity profiles in the right upper lobar bronchus (Station 10). Inspiratory flow at two flow rates.

deal more momentum, it was able to overcome the adverse pressure gradient near the outside wall of the sharp bend.

EXPIRATORY FLOW

Expiratory flow velocity profiles in Stations 11, 12, 9 and 5 are shown in fig. 9. Unlike in the case of inspiratory flow, the velocity profiles entering the five lobar bronchi during expiratory flow could not be well regulated. Thus at the low flow rate of 0.4 L/sec the profiles at Stations 11 and 12 were somewhat parabolic, but at 1.7 L/sec they were more or less flat. As the air entered the distal portion of the right main bronchus (Station 9) from the two branches, the velocity profiles in the frontal plane (A–A′) had a sharp peak near the center and those in the sagittal plane (C–C′) were much flatter. These characteristics were stronger at 0.4 L/sec than at 1.7 L/sec and they are at least qualitatively consistent with the observations

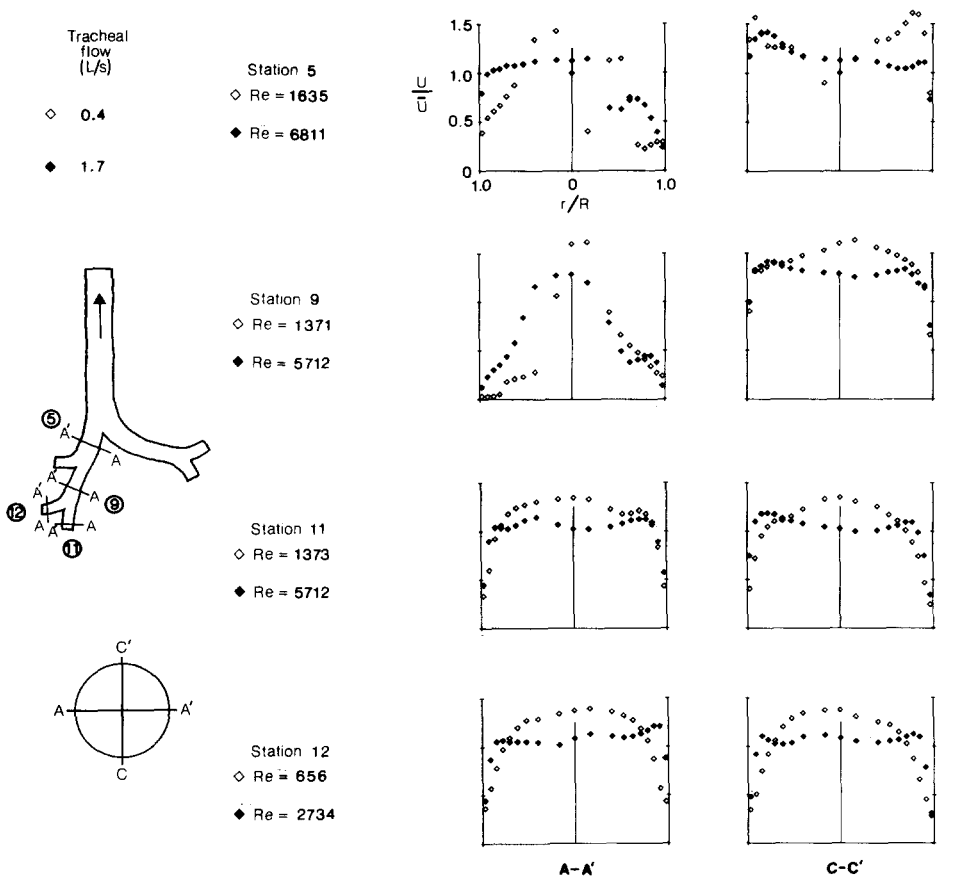

Fig. 9. Axial velocity profiles in the right lung (Stations 5,9,11,12). Expiratory flow at two flow rates.

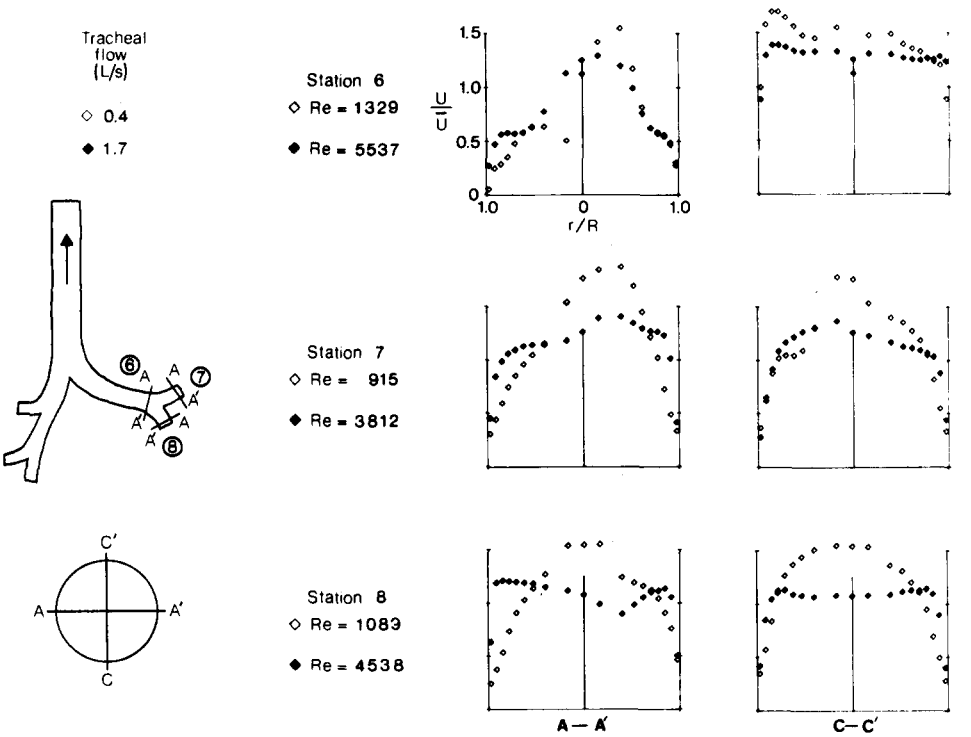

Fig. 10. Axial velocity profiles in the left lower (Station 8) and upper (Station 7) lobar bronchi as well as in the distal part of left main bronchus (Station 6). Expiratory flow at two flow rates.

of Schroter and Sudlow (1969). Joined by air coming from right upper bronchus (Station 10, not shown), the air reached the proximal position (Station 5) of right main bronchus with uneven and fairly complicated profiles. Probably due to a slight variation in the alignment of the resistors and the airways during two different measurements, the profiles at Station 5 for the two flow rates were quite different and neither was symmetrical. The frontal profiles were skewed toward the inner wall of the bifurcation or outer wall of the bend.

Figure 10 shows the profiles in the left lung model. Again the entering profiles (Stations 7 and 8) were nearly parabolic at the lower flow rate 0.4 L/sec and were much flatter at the higher flow rate. As the fluid merged in the left main bronchus (Station 6) the profiles were qualitatively similar to those observed at Station 5, namely, skewed frontal profile leaning toward the inner wall of the bifurcation and blunter and nearly flat profiles in the sagittal plane.

A complete and very different set of profiles obtained at Station 4, some 3 diameters downstream from Station 6, are presented in fig. 11. While the profiles in the frontal plane at Station 6 had a single peak near the center, the present profiles exhibited two peaks near the wall. These peaks are more moderate at the higher flow rate, but are nonetheless independent of flow rate in their basic configuration.

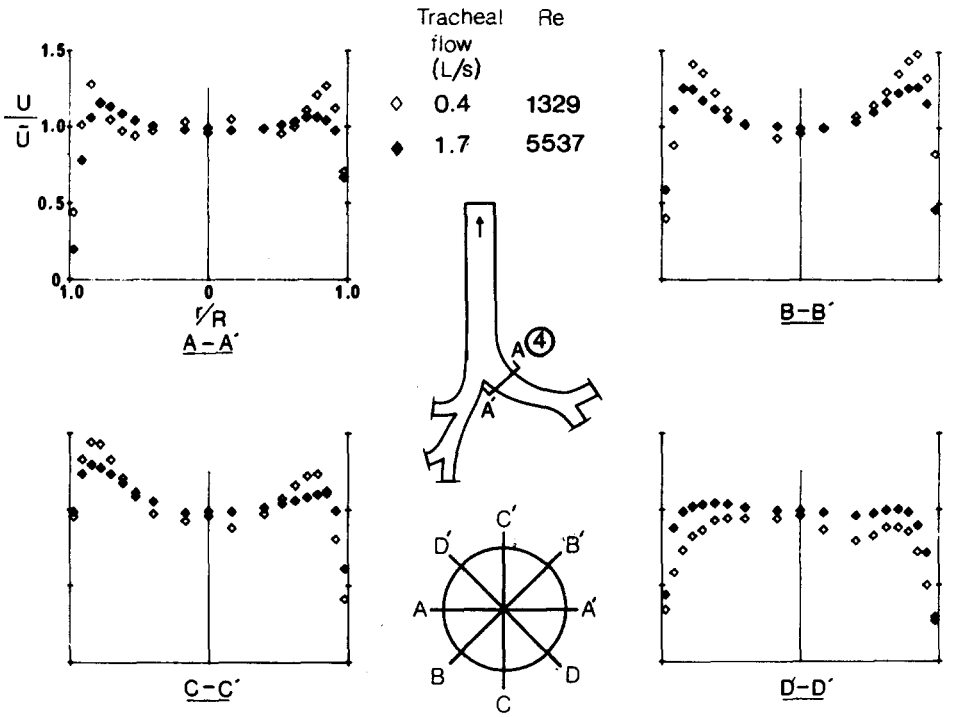

Fig. 11. Axial velocity profiles along 4 diameters in the proximal part of the left main bronchus (Station 4). Expiratory flow at two flow rates.

The interesting feature is the changes which occur over a distance of 3 diameters in this curved airway. Schroter and Sudlow (1969) measured expiratory velocity profiles after a single bifurcation only up to 2 diameters downstream of the bifurcation; their profiles were qualitatively similar to our profiles at Stations 9 and 6. The very different profiles at Station 4 appear to indicate that there was considerable secondary flow in this airway branch and that the secondary flow probably played a role in modifying the axial flow profiles.

As the air merged in the trachea, the axial velocity profiles (fig. 12) took the basic shape of those after a single bifurcation: a peak in the frontal plane and nearly flat in the sagittal plane. Since the right and left main bronchi join the trachea from different angles, the velocity profiles were not symmetric but skewed toward the right wall. In other words, the influence of the curvature came mainly from the left main bronchus. Perhaps because the trachea is straight, velocity profiles at Station 1 (not shown) were not very different from those at Station 2, namely, the type of change observed between Station 6 and Station 4 did not appear in the trachea.

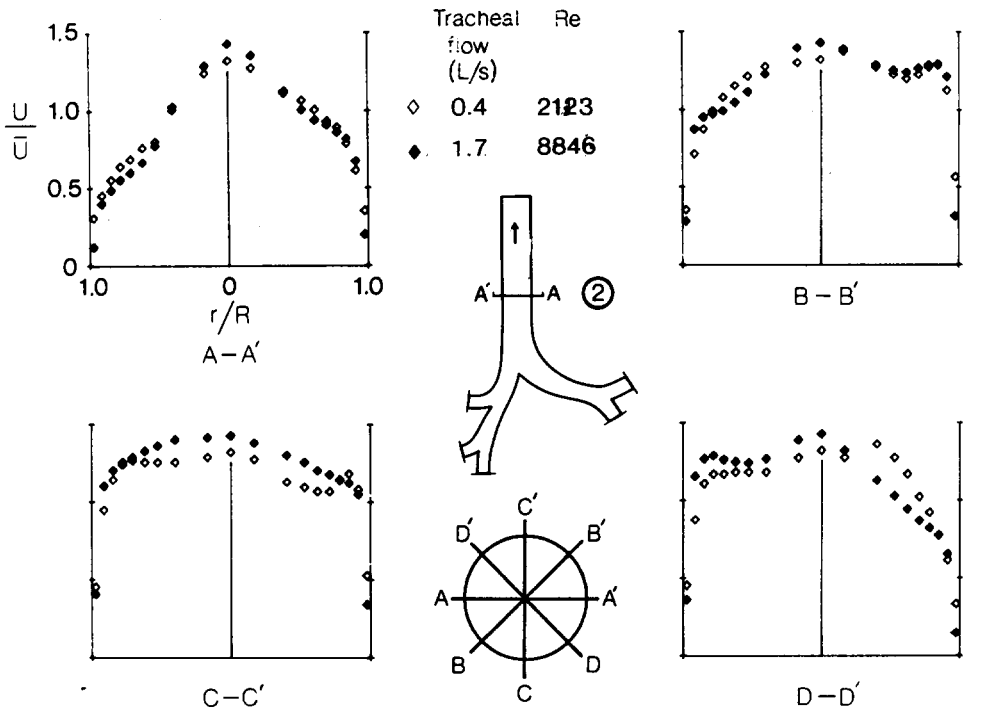

Fig. 12. Axial velocity profiles along 4 diameters in the trachea (Station 2). Expiratory flow at two flow rates.

Discussion

MODEL GEOMETRY

In studying air flow dynamics in the tracheo-bronchial tree one is usually confronted with a choice between ease of measurement and realistic airway geometry. Schroter and Sudlow (1969) and Schreck and Mockros (1970) used easily accessible models of highly idealized geometry. Olson *et al.* (1973), on the other hand, used a real-size lung cast, thus were unable to make detailed velocity measurements. In the present study we attempted to solve the above dilemma by employing a specially constructed 3:1 scale model of the human central airways. This approach enabled us to work with an essentially correct airway geometry and at the same time make detailed measurements.

Our model, however, was still idealized in that it was rigid, dry and with smooth walls. The justification for using this kind of model has been discussed by Schroter and Sudlow (1969). Here we shall deal with these points briefly in the light of our current perspective.

In normal quiet breathing, the length and diameter variations of the large airways are quite moderate (Hughes *et al.*, 1972), and the rate of these variations is much

smaller compared to the linear velocity of air. Thus, under such circumstances, the influence of wall movement on air flow dynamics is likely to be minimal. In deep and rapid breathing, or in airways much smaller than those which we studied, wall movement could conceivably play a role in modifying the flow patterns in the airways.

The airways are generally lined with a thin layer of mucus. Although the air–liquid interface would seem to differ from the air–solid wall interface in terms of viscous dissipation, this has not been bound to be the case when the breathing frequency is low, air flow rate is moderate, and the mucus lining is not excessively thick (King *et al.*, 1982). These authors have reported that the introduction of a mucus lining in a dry tube causes no significantly greater viscous pressure drop beyond that which is caused by the mere constriction of the tube. Therefore, the presence of liquid lining *per se* is not expected to alter velocity profiles in the airways.

The omission of cartilage rings in the interior wall of large airways was more problematic. The local velocity gradients would likely be altered if the model had corrugations. On the other hand, we were more interested in the general shape of the velocity profiles than the local velocity gradients or wall shear stresses. Since it is exceedingly difficult to manufacture a model with realistic corrugation to simulate the cartilage rings, and since our hot-wire probe was not small enough to render accurate readings within 1 mm of the wall, we decided to use a smooth-walled model at the cost of accurate information on local velocity gradients.

STEADY AND QUASI-STEADY FLOWS

We used steady flow in this study. An unsteady or oscillatory flow may be dynamically approximated by a steady flow if certain criteria are met. These criteria have been discussed by Schroter and Sudlow (1969), Jaffrin and Kesic (1974), Pedley *et al.* (1977), and more recently, Isabey and Chang (1981). Among the various parameters discussed by these authors, two are probably most significant in governing the behavior of flow in the airways.

The most commonly used parameter is Womersley number

$$\alpha = \frac{d}{2}\sqrt{\frac{\omega}{\nu}} \tag{4}$$

in which d is the diameter of the tube and ω the angular frequency of an oscillatory flow. Originally derived for a fully developed laminar flow in a straight circular tube, this parameter gives the relative importance of the viscous forces in a fluid flow to the inertia forces due to local acceleration. It depends on airway geometry, fluid property and frequency of oscillation, but is independent of flow rate. If α is much greater than unity, the flow is definitely unsteady; conversely, an unsteady flow could be considered quasi-steady. At quiet and moderate breathing frequencies values of α in the central airways are not much greater than unity. However, at a frequency of 2 Hz, values of α in the first three generations of airway vary between

2.4 and 7.3, indicating that velocity profiles obtained during steady flows are probably no longer representative of the true velocity profiles.

A more pertinent parameter is one which contains the flow rate as well as an accelerative inertia term. Isabey and Chang (1981) employed

$$\varepsilon = \frac{\omega L \dot{U}}{U^2} \tag{5}$$

where L is the length of an airway, U is mean linear velocity in this airway and $\dot{U}$ is the local acceleration or time derivative of U. Physically, ε signifies the relative magnitude of local acceleration to connective acceleration in a flow. It is clear from eq. (5) that, during an oscillatory flow cycle, ε becomes very large near zero flow or flow reversal and attains minimal values at the two peak flows. In other words, the velocity profiles at certain portions of a breathing cycle may be quite satisfactorily represented by the steady velocity profiles; however, at points near flow reversal, inertia effects make the velocity profiles much flatter than those found in this study during steady flow.

In view of the recent interest in high frequency ventilation as well as the measurement of respiratory resistance by means of forced oscillations, a full investigation of the velocity profiles at various phases of an oscillatory cycle has been undertaken in our laboratory and will be reported as a sequel to the present study (Menon *et al.*, 1982).

PRINCIPAL FINDINGS

The major findings of this study may be summarized as follows: by using a realistic central airway model we have corroborated the pioneer work by Schroter and Sudlow (1969) in a qualitative manner; we have also obtained quantitative data not reported by previous workers.

During inspiratory flow, the velocity profiles are mainly shaped by the carina and the curvature of the airways. The basic features of these velocity profiles are quite independent of the Reynolds numbers of the flow. Thus, in the frontal plane the velocity profiles usually showed a high degree of asymmetry with peak velocities near the outer wall of the bend. In the sagittal plane the velocity profiles were generally symmetric, with a bi-peak structure in most instances. When the airway branching did not involve a sharp curvature (Stations 5 and 9) such bi-structures were less evident.

During expiratory flow the velocity profiles were nearly symmetric, exhibiting a single peak near the center in the frontal plane and almost flat in the sagittal plane. Again, these basic features were largely independent of Reynolds number but very dependent on the local geometry.

Since the axial velocity profiles are very sensitive to model geometry, the importance of studying a realistic model is thus underscored. In the model we studied,

only at one location (Station 10) was flow separation observed, although the possibility of such occurrence has been raised by various authors (Schroter and Sudlow, 1969; El Masry *et al.*, 1978). Since flow separation is known to cause large amount of energy dissipation, our present finding should therefore have some relevance on the theoretical study of airway resistance.

In terms of deposition of inhaled particles, the right upper lobar bronchus (Station 10) is also a more likely site than the other branches because separation causes fluid retardation. However, except by the mechanism of impaction due to secondary flow velocities, there is little reason to suggest that airborne particles are likely to deposit in the central airways because the axial momentum is in general very large.

We studied a standard flow distribution (table 3) plus an altered distribution due to added resistance in one lobe. We demonstrated that variation in flow distribution did not greatly alter the axial velocity profiles (fig. 7), just like the two flow rates used generated mostly similar profiles at the corresponding sites.

By using a full round opening and a narrow slit at the tracheal entrance, we attempted to determine the effect of the glottic aperture on flow patterns in the airways. We found that despite very different velocity profiles in the trachea (fig. 3) the velocity profiles in the main bronchi due to these two entrance conditions were not very different (fig. 4). Thus it would seem that flow patterns in the bronchial tree are little affected by such factors as vagal stimulation, phonation, or the resting geometry of the upper airways.

When we compared expiratory flow profiles at Station 6 and Station 4, we found an unexpected evolution in the curved left main bronchus. The velocity profiles changed from a single peak structure at Station 6 to a bi-peak structure at Station 4. This evolution was not observed in the trachea (from Station 3 to Station 1) during the same expiratory flows, neither has it been reported by any of the previous authors, none of whom utilized a curved daughter branch in their studies. Since this evolution occurred at two flow rates and was highly repeatable, we could not but acknowledge its validity and attribute it to the influence of secondary flow in the left main bronchus.

Acknowledgements

The authors are indebted to Mr. Albert Hagemann for his skillful and artistic manufacturing of the model used in this study. This study was supported by the Medical Research Council of Canada.

References

Daily, J. W. and D. R. F. Harleman (1966). Fluid Dynamics. New York, Addison-Wesley.

El Masry, O. A., I. A. Feuerstein and G. F. Round (1978). Streamlines and separated flows in branches. *Circ. Res.* 43: 608–618.

Horsfield, K., G. Dart, D. E. Olson, G. F. Filley and G. Cumming (1971). Models of the human bronchial tree. *J. Appl. Physiol.* 31: 207–217.

Hughes, J. M. B., F. G. Hoppin, Jr. and J. Mead (1972). Effect of lung inflation on bronchial length and diameter in excised lungs. *J. Appl. Physiol.* 32: 25–35.

Isabey, D. and H. K. Chang (1981). Steady and unsteady pressure–flow relationships in the central airways. *J. Appl. Physiol.* 51: 1338–1348.

Isabey, D. and H. K. Chang (1982). A model study of flow dynamics in human central airways. Part II: Secondary flow velocities. *Respir. Physiol.* 49: 97–113.

Jaffrin, M. Y. and P. Kesic (1974). Airway resistance: a fluid mechanical approach. *J. Appl. Physiol.* 36: 354–361.

King, M., H. K. Chang and M. E. Weber (1982). The resistance of mucus lined tubes to steady and oscillatory air flow. *J. Appl. Physiol.* 52: 1172–1176.

Menon, A., M. E. Weber and H. K. Chang (1982). A model study of flow dynamics in human central airways. Part III: Oscillatory velocity profiles (Manuscript).

Olson, D. E. (1971). Fluid mechanics relevant to respiration: flow within curved or elliptical tubes and bifurcating systems. Ph. D. thesis, Imperial College, London.

Olson, D. E., M. F. Sudlow, K. Horsfield and G. F. Filley (1973): Convective patterns of flow during inspiration. *Arch. Intern. Med.* 131: 51–57.

Pedley, T. J., R. C. Schroter and M. F. Sudlow (1977). Gas flow and mixing in the airways. In: Bioengineering Aspects of the Lung, edited by J. B. West. New York, Marcel Dekker, pp. 163–265.

Schreck, R. M. and L. F. Mockros (1970). Fluid dynamics in the upper pulmonary airways. AIAA 3rd Fluid and Plasma Dynamics Conference, Los Angeles, California.

Schroter, R. C. and M. F. Sudlow (1969). Flow patterns in models of the human bronchial airways. *Respir. Physiol.* 7: 341–355.